Land surface temperature retrieved from SEVIRI/MSG2 data: algorithm and validation

Mariam Atitar, José Antonio Sobrino, Guillem Soria, Jean-Pierre Wigneron, Juan Carlos Jiménez-Muñoz, Yves Julien, Ana Belen Ruescas

LAND SURFACE TEMPERATURE RETRIEVED FROM SEVIRI /MSG2 DATA: ALGORITHM AND VALIDATION

M. Atitar[1], J.A. Sobrino[1], G. Soria[1], J.P. Wigneron[2], J.C. Jiménez-Muñoz[1], Y. Julien[1], A. Belen Ruescas[1]

[1] Department of Earth, physics, and Thermodynamics, University of Valencia, Burjassot, 46100, Valencia. Spain
[2] INRA, Institut National de la Recherche Agronomique, Bordeaux-Aquitaine, B.P. 81, 33883 Villenave d'Ornon Cedex, FRANCE

***Abstract*—The main purpose of this paper is to give an operational algorithm for retrieving the land surface temperature (LST) using the Spinning Enhanced Visible and Infrared Imager (SEVIRI) data on board of MSG2 (Meteosat Second Generation) Satellite. The algorithm is a split window method using the two thermal infrared channels (IR10.8 and IR12.0). MODTRAN 4.0 code was used to obtain numerical coefficients of the algorithm proposed. The results show that the algorithm is capable to produce LST with a standard deviation of 0.7K and a root mean square error (RMSE) of 1.3K, both of them, for viewing angle lower than 50º. The algorithm has been applied to a series of MSG2 images obtained from a MSG antenna system installed at the IPL (Image Processing Laboratory) in the University of Valencia. The LST product has been validated using in situ data from an ESA (European Space Agency) field campaign named CEFLES2 (CarboEurope, FLEx and Sentinel-2) carried out in 2007 in Bordeaux (France) and MODIS LST products over different surfaces and under different viewing angles. The results show a RMSE of 1.9K for in situ data, and the comparison with MODIS LST products shows a RMSE of 1.2K.**

***Index Terms*— Land surface temperature (LST), Meteosat second generation (MSG), Spinning Enhanced Visible and Infrared Imager (SEVIRI), Split window (SW)**

I. INTRODUCTION

Meteosat Second Generation (MSG) satellite was jointly developed by European Space Agency (ESA) and EUMETSAT. The last satellite of MSG 2 series (Meteosat 9) was launched in December 2005. MSG satellite's main payload is the Spinning Enhanced Visible and Infrared Imager (SEVIRI). This optical imaging sensor detects radiation in 12 spectral channels; three visible and near-infrared channels are centered at 0.6, 0.8 and 1.6 µm, and eight infrared channels centered at 3.9, 6.2, 7.3, 8.7, 9.7, 10.8, 12.0 and 13.4 µm, and finally one visible broadband channel (HRV) at 0.5-0.9 µm. The maximum dynamic range for the 3.9, 10.8 and 12.0 µm channels is 335K according to [15]. Another advantage of MSG satellite, that it provides diurnal coverage with a match higher temporal resolution (15 minutes) in comparison with orbital satellites. LST exhibits strong diurnal variation which cannot be captured by a single polar orbiting satellite. All these features make SEVIRI very attractive for surface temperature retrieval.

In order to retrieve the LST algorithm from SEVIRI/MSG2 data, we propose in this paper a new split window algorithm that uses the thermal bands IR10.8 and IR12.0. This algorithm takes into account the SEVIRI angular dependence.

The split-window coefficients are derived from the MSG2 forward simulations with the moderate resolution atmospheric radiance and transmittance model (MODTRAN 4.0), following to [1] and [2].

II. SPLIT WINDOW ALGORITHM

The structure of the algorithm was obtained from the radiative transfer equation, considering the at-sensor radiance, $B(T_{i\theta})$ at-sensor, for a given channel i and under a zenith observation angle θ according to:

$$B(T_{i\theta}) = \varepsilon_{i\theta} B_i(T_s)\tau_{i\theta} + R^{\uparrow}{}_{ati\theta} + R_i(ref)\tau_{i\theta} \qquad (1)$$

where: $\varepsilon_{i\theta}$ is the surface emissive, $B_i(T_s)$ is the radiance emitted by a blackbody at temperature T_s of the surface, $R_i(ref)$ is the reflected atmospheric radiance given by Eq.2:

$$R_i(ref) = R^{\downarrow}_{ihem}(1-\varepsilon_{i\theta}) \qquad (2)$$

where $R^{\downarrow}_{ihem}$ is the dowelling atmospheric radiance from the whole hemisphere in channel i, which can be obtained directly from MODTRAN 4.0 simulation, together with the atmospheric upwelling radiance Ratio and the total atmospheric transmittance $\tau_{i\theta}$. More details can be found in [10]. The structure of the LST algorithm is given by [6] and adapted in this case to SEVIRI data:

$$\begin{aligned} T_s &= T_i + a_1(T_i - T_j) + a_2(T_i - T_j)^2 + a_3(1-\varepsilon) \\ &+ a_4 W(1-\varepsilon) + a_5\Delta\varepsilon + a_6 W\Delta\varepsilon + a_0 \end{aligned} \qquad (3)$$

where T_s is the surface temperature (in K), T_i and T_j are the at-sensor brightness temperatures of two SEVIRI thermal channels (in K), ε is the mean effective emissive $\varepsilon = (\varepsilon_i + \varepsilon_j)/2$, Δε is the emissive difference $\Delta\varepsilon = \varepsilon_i - \varepsilon_j$, W is the total atmospheric water vapor ($g.cm^{-2}$), in the direction of observation and a_i are the numerical coefficients of the algorithm.

III. Methodology

A. Simulated data

As we indicated before, The MODTRAN 4.0 code has been used to extract the coefficients of the two channel algorithm and analyze the atmospheric effects, in this end, a set of two radiosondes observation databases were considered: 61 radiosondes observations extracted from the TOVS initial guess retrieval (TIGR) data base [5], which covered a wide range of atmospheric and surface conditions, and the standard atmospheric profiles defined in MODTRAN such as mid latitude summer, mid latitude winter, tropical, south arctic summer, and south arctic winter.

Considering the angular variation of SEVIRI, seven viewing zenith angles were used in the simulations (0º, 10º, 20º, 30º, 40º, 50º, 60º). Another important parameter in these simulations is the emissivity; therefore, with the absence of angular values of emissive, we have selected 108 emissive spectra from the ASTER library at nadir. For each thermal channel, the values of emissivity were obtained by integration of the filter response function, with the appropriate emissivity spectrum.

As a result, we had 46116 different geophysical situations (61 atmospheres, 7 angles and 108 emissivity spectra) for each thermal channel. The emissivities calculated can be observed in Fig. 1, with a range from 0.7 to 0.99. The atmospheric water vapor at nadir was extracted from the 61 radiosoundings of the TIGR database, providing a range of (0–6) ($g.cm^{-2}$) for the simulations.

B. MSG data

MSG data used in the present work have been acquired at the Image Processing Laboratory (IPL) of the University of Valencia. More details about the radiometric correction and data calibration are made in the appendix. The emissivity values are calculated following to [8] and the total atmospheric water vapor is calculated according to [13].

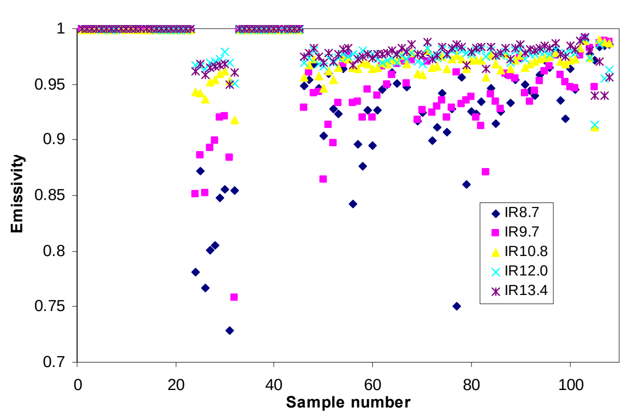

Fig.1. Filtered emissivity values for the five SEVIRI thermal channels

IV. Results and Discussions

A. Algorithm coefficients and sensitivity analysis:

In this section we present the final LST algorithm, and the study of its sensitivity. In order to obtain the numerical values of the coefficients, the MODTRAN outputs and the emissivity spectra are used in eq.5. The results of using the least square minimization procedure to calculate the standard deviation and choose the best combination of the two thermal channels are shown in table.1. IR10.8 and IR12.0 give the minimum standard deviation, 0.35K at nadir and 1.6K at 60º.

Table I
Standard deviation (K) of the LST Algorithm using different SEVIRI two thermal channels combinations and 7 zenith observations angles

Ch. i	Ch. j	0º	10º	20º	30º	40º	50º	60º
IR 8.7	**IR 9.7**	1.428	1.442	1.483	1.559	1.692	1.889	2.68
IR 8.7	**IR 10.8**	1.424	1.438	1.484	1.567	1.712	1.937	3.034
IR 8.7	**IR 12.0**	1.048	1.059	1.093	1.158	1.278	1.53	2.772
IR 8.7	**IR 13.4**	0.685	0.694	0.721	0.771	0.861	0.997	1.786
IR 9.7	**IR 10.8**	1.459	1.476	1.529	1.625	1.789	2.029	3.102
IR 9.7	**IR 12.0**	2.024	2.043	2.103	2.209	2.383	2.631	4.107
IR 9.7	**IR 13.4**	4.35	4.398	4.547	4.824	5.254	5.726	8.131
IR 10.8	**IR 12.0**	**0.348**	**0.354**	**0.375**	**0.416**	**0.5**	**0.69**	**1.608**
IR 10.8	**IR 13.4**	1.116	1.134	1.192	1.297	1.457	1.719	2.451
IR 12.0	**IR 13.4**	1.799	1.822	1.893	2.018	2.199	2.483	3.608

Therefore, table 2 shows the coefficients for the LST algorithm using the two thermal channels IR10.8 and IR12.0 based on the viewing zenith angles.

Table II
Numerical Values of the Coefficients of the LST Algorithms

θ (º)	a_1	a_2 (K^{-1})	a_3 (K)	a_4 ($cm^2.K.g^{-1}$)	a_5 (K)	a_6 ($cm^2.K.g^{-1}$)	a_0 (K)
0	1.21	0.36	49.28	-4.23	-105.05	15.06	0.23
10	1.21	0.37	49.11	-4.13	-105.03	14.85	0.24
20	1.20	0.38	48.56	-3.83	-105.00	14.23	0.27
30	1.18	0.40	47.45	-3.29	-105.12	13.25	0.33
40	1.16	0.44	44.69	-2.33	-105.44	11.96	0.45
50	1.20	0.47	39.57	-1.02	-108.74	10.87	0.66
60	0.85	0.60	18.72	3.30	-55.03	1.57	2.00

Table 3. shows the estimation errors and the total errors obtained by the database for each observation angle ($\sigma_{total} = \sqrt{\sigma_{Sd}{}^{2} + \sigma^{2}{}_{noise} + \sigma^{2}{}_{\varepsilon} + \sigma^{2}{}_{W}}$), where σ_{total} is the total error for all the simulated database (in K), σ_{Sd} is the standard error of the estimation (in K) given in table 3, σ_{noise} is the uncertainty due to the noise equivalent delta temperature (in K), σ_{ε} is the uncertainty due to the error on the surface emissivity (in K),

σ_w is the uncertainty due to the error on the atmospheric water vapor (in K) and r is the correlation coefficient.

TABLE III
ESTIMATIONS ERRORS AND THE TOTAL ERROR OBTAINED BY THE DATABASE SIMULATIONS BASED ON THE VIEWING ZENITH ANGLES

θ(º)	σ_{Sd}	r	σ_{noise}	σ_{ε}	σ_w	σ_{total}
0º	0.348	0.983	0.372	0.972	0.12	1.103
10º	0.354	0.982	0.374	0.971	0.118	1.105
20º	0.375	0.982	0.381	0.968	0.111	1.112
30º	0.416	0.98	0.394	0.965	0.101	1.127
40º	0.5	0.976	0.416	0.96	0.083	1.162
50º	0.69	0.965	0.446	0.965	0.064	1.269
60º	1.608	0.869	0.459	0.734	0.037	1.826

B. The proposed algorithm

In order to give a general algorithm for the LST, we have fit the coefficients given in table 2 with a function based on the satellite observation angle. Eq. 4 gives the physical algorithm that we propose to obtain LST from SEVIRI/ MSG2 data, where θ is the satellite zenith observation angle.

The water vapor values necessary for the LST calculations were obtained following to [4] and [13], and the channel emissivity has been estimated using the threshold method developed in [8] and adapted to SEVIRI data. Another LST algorithm was developed in [12] and it's adapted to MSG1 data.

$$\begin{aligned} T_s &= T_{IR10.8} + \left[1.34 - \frac{0.11}{\cos^2(\theta)}\right](T_{IR10.8} - T_{IR12.0}) \\ &+ \left[0.29 + \frac{0.08}{\cos^2(\theta)}\right](T_{IR10.8} - T_{IR12.0})^2 + \left[60.67 - \frac{10.01}{\cos^2(\theta)}\right](1-\varepsilon) \\ &+ \left[-6.71 + \frac{2.47}{\cos^2(\theta)}\right]W(1-\varepsilon) + \left[-125.91 + \frac{15.09}{\cos^2(\theta)}\right]\Delta\varepsilon \\ &+ \left[19.44 - \frac{4.27}{\cos^2(\theta)}\right]W\Delta\varepsilon + \left[-0.44 + \frac{0.57}{\cos^2(\theta)}\right] \end{aligned} \tag{4}$$

V. VALIDATION

A. Validation with in situ data

A validation of the LST product has been carried out using datasets collected from a field campaign carried out in the zone of Bordeaux (44º43'01.7''N, 0º46'09.8''W). Since 26th, April 2007, two radiometers (Raytek and Everest) have been installed in a tower of 33 meters of altitude, in the forest zone of Le Bray (Bordeaux). The two radiometers are oriented at nadir with a field of view (FOV) of 6º and 4º respectively, they had a single band 8-14 μm and they measure every 5 minutes.

The date selected to compare the LST products is 27th, July 2007, a cloud-free day. SEVIRI products were compared with the in situ data. Figure 2 shows the outputs of the algorithm proposed in this paper, in comparison with temperature obtained from the two radiometers Raytek (R) and Everest (EV) brightness temperature. The forest emissivity value considered was 0.98.

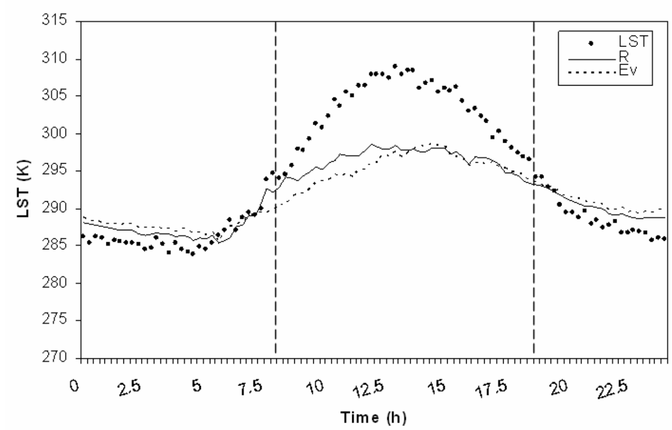

Fig.2. SEVIRI LST and temperatures measured by the two radiometers Raytek and Everest, during July, 27th 2007

The comparison of the data includes 96 SEVIRI images, acquired every 15 minutes, during the selected day. Effective temperatures were averaged every 15 minutes in order to compare them with LST calculations.

The comparison between temperatures given from in situ data and LST given by the algorithm proposed is given in Table 4. In the afternoon and in the night, the RMS (root mean square) error is lower than 1.9K, but during the day the RMSE is up to 7.6 K. This is due to the scale factor between the surface mapping by the radiometers (16mx16m) and the pixel SEVIRI (3kmx3km), thus, in the pixel SEVIRI there are included others surfaces in addition to the forest area (bare soli, road,etc), and these cause that the measurement is less representative in the central hour of the day when there is a high thermal heterogeneity, which explains the difference between the measures in situ and the SEVIRI LST during the day between 8h30 and 18h15 UTC. Beside, we include in this paper a second validation using LST of MODIS.

TABLE IV
ROOT MEAN SQUARE ERRORS OF THE COMPARISON BETWEEN LST AND RADIOMETERS RAYTEK1 (R) AND EVEREST (EV) DURING JULY, 27TH

Time	$T_{SEVIRI} - T_{EV}$ (K)	$T_{SEVIRI} - T_R$ (K)
0h - 8h30	1.88	1.02
8h30 - 18h15	7.6	6.6
18h30 - 23h45	1.66	1.13

B. Validation with MODIS data

In order to check latitude and longitude influence and surface type, the LST proposed in this paper was compared with LST calculated from MODIS data, using the algorithm developed in [7]; Eq.15 gives the expression of this algorithm:

$$T_s = T_{31} + 1.02 + 1.79(T_{31} - T_{32}) + 1.2(T_{31} - T_{32})^2 + (34.83 - 0.68W)(1-\varepsilon) + (-73.27 - 5.19W)\Delta\varepsilon \qquad (5)$$

where the emissivity and water vapour values were calculated following to [7].

The day selected to compare the SEVIRI LST is 27th, July 2007 at 11:00 UTC. The comparison of the products was carried out in four different and homogenous areas of 3x3 pixels of SEVIRI that equal to 9x9 MODIS pixels. Figure 3 shows the SEVIRI LST image with the four test areas, and table 5 shows the difference between the two products in the four areas and under different viewing angles.

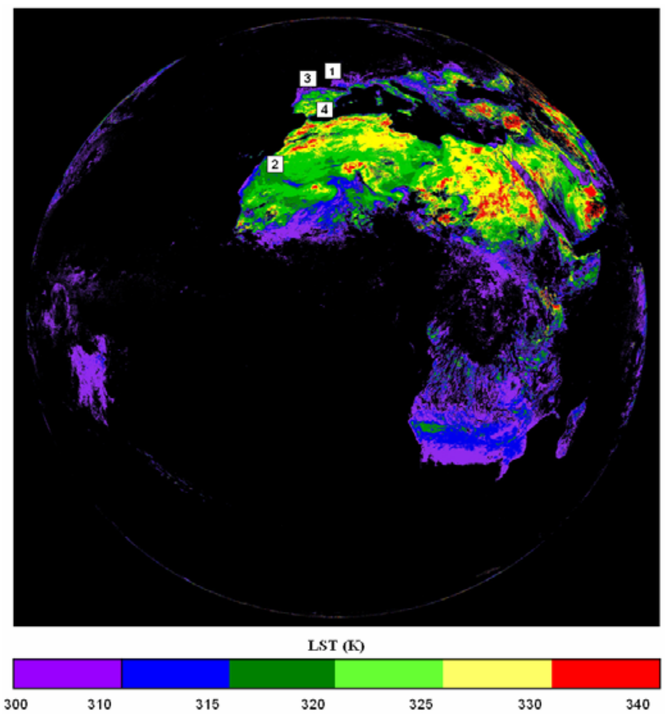

Fig.3. SEVIRI LST image for July, 27th 2007 at 11:00 UTC and test areas

TABLE V
DIFFERENCE BETWEEN THE LST ALGORITHM ESTIMATED FROM SEVIRI AND THE MODIS PRODUCT IN FOUR DIFFERENT AREAS AND AT DIFFERENT VIEWING ANGLES

Zone	Latitude	Longitude	Viewing Angle (º)	T_{Modis}- T_{seviri} (K)
1. Le bray (France)	44º 42’ 47.26’’N	0º 46’ 30.27’’W	51	1.14
2. Desert (Morocco)	28º 59’ 28.92’’N	6º 09’ 21.39’’W	34	-1.53
3. Vegetation (Spain)	42º 16’ 40.84’’N	8º 24’ 37.40’’W	50	-0.65
4. Mediterranean Sea	36º 10’ 12.95’’N	4º 02’ 29.83’’W	41	0.15

In general, the LST products of SEVIRI and LST products of MODIS give similar results. The standard deviation of this comparison is about 1.14K and the total RMSE is about 1.16K. These values are in the range of the algorithm error, and therefore, they give confidence about the performance of the LST algorithm retrieving from SEVIRI/MSG2 data.

VI. CONCLUSION

In this paper, we present an operational algorithm to retrieve LST from SEVIRI data. From the simulations, it is shown that LST can be obtained with an error of 1.3 at viewing angles lower than 50º. LST products have been validated using in situ data and LST products from MODIS.

APPENDIX

At the Image Processing Laboratory Satellite Data in the University of Valencia, The MSG SEVIRI data are received near real time through the mandatory TELLICAST client software [11]. Further file handling is carried out using the Dartcom XRIT Ingester software, which automatically acquires decrypts, decompresses and archives raw HRIT (High Resolution Information Transmission) data, and then outputs are ready for display and further processing. HRIT image is a PGM (Portable Gray Map) format, which is a lowest common denominator grayscale file format coding in 10 bits, it is designed to be extremely easy to learn and write programs. For the quantitative exploitation, MSG data have to be calibrated in reflectance and brightness temperature. The calibration relation is given by:

$$R = (Slope * DN) + Offset \qquad (6)$$

where R is the radiance in $mWm^{-2}sr^{-1}(cm^{-1})^{-1}$, DN is the digital MSG2 count; Image calibration slope and offset are read from the image header information, typical values of slopes and offsets are given in Table 6, for the four channels used in this study:

TABLE VI
SLOPES AND OFFSETS FOR MSG2 CHANNELS

Channels	Slope	Offset
VIS06	0.02014	-1.02691
VIS08	0.02592	-1.32202
TIR10.8	0.20503	-10.45676
TIR12.0	0.22231	-11.33788

To calculate reflectance from radiance, the following relation ship is used:

$$\rho = \frac{\pi * R * d_{SA}{}^2}{I * \cos(\theta)} \qquad (7)$$

where ρ is the bidirectional Reflectance Factor (BRF) and d_{SA} is the Sun-Earth distance in Astronomic Unit (AU), at time t, its value is given by:

$$d_{SA} = 1 - 0.0167 \cos\left(\frac{2\pi(JulianDay - 3)}{365}\right) \qquad (8)$$

where I is the Band solar irradiance at 1 AU in $mWm^{-2}(cm^{-1})^{-1}$, for VIS06 channel: I = 65.2065 $mWm^{-2}(cm^{-1})^{-1}$ and for VIS08 channel: I = 73.1869 $mWm^{-2}(cm^{-1})^{-1}$, according to [14], and finally, θ is the solar zenith Angle in Radians.

The thermal channel radiances may be converted into brightness temperatures as follow:

$$T_b = \frac{c_2 \nu_2}{\left(\log\left(\frac{c_1 \nu_c^3}{R} + 1\right) - B\right) * A} \tag{9}$$

where T_b is the equivalent brightness temperature in K, $\mathbf{v_c}$ is the wave number (in cm^{-1}), A and B are constants given in table 7, and finally C_1 and C_2 are the radiation constants, which values are: C_1=1.1910659.10^{-5} $mWm^{-2}Sr^{-1}(cm^{-1})^{-4}$ and C_2= 1.438833 cm.K:

TABLE VII
A, B AND THE CENTRAL WAVE NUMBERS FOR THE TWO THERMAL CHANNELS IR10.8 AND IR12.0

Channels	ν_c	A	B
TIR10.8	930.659	0.9983	0.627
TIR12.0	839.661	0.9988	0.397

ACKNOWLEDGMENT

This work was carried out while Mariam Atitar was in receipt of a grant from the AECI ‘Agencia Española de Cooperación Internacional’. We wish to thank the European Space Agency ESA-ESTEC (CEFLES2 project) for providing us in situ data and INRA (Institut National de la Recherche Agronomique - Bordeaux - France)), especially Mr. Jean-Marc Bonnefond who carries out the recurring download of in situ data

We wish to thank the Ministerio de educación y ciencias for financing the SEVIRI antenna project (ESP-2005-24355-E and UNLOV05-23-004), and TERMASAT project (ESP-2005-07724-C05-04)

REFERENCES

[1] Abreu, L W. and Anderson G.P (Eds.). (1996). The MODTRAN 2/3 Report and LOWTRAN 7 MODEL, MODTRAN report, Contract F19628-91-C-0132

[2] Berk, A., Bernstein, L. S., Anderson, G. P., Acharya, Robertson, D. C., Chetwynd, J. H., and Adler-Golden, S. M. (1998). MODTRAN cloud and multiple scattering upgrades with application to AVIRIS. Remote Sensing of Environment, 65, 367−375.

[3] Carlson, T.N. and Ripley, D.A. (1997). On the relation between NDVI, fractional vegetation cover, and leaf area index, Remote Sensing of Environment, 62, 241-252

[4] Schroedter-Homscheidt, M., Bugaliaro, L. Erbertseder, T., Gesell, G. And Holzer-Popp, T. (2004a), Report on atmospheric parameter retrieval, Enery-Specific Solar Radiation Data from Meteosat Second Generation (MSG): The Heliosat-3 Project (Contract NNK5-CT-2000-00322), 31 May 2004, DLR

[5] Scott, N.A. and Chedin, A. (1981). A fast line by line method for atmospheric absortion computations; the automatized Atmospheric Absortion Atlas. Journal of Meteorology, 20, 802-812

[6] Sobrino, J.A, Z.-L.Li, Stoll, M.p. and Becker, F. (1996). Multi.Channel and Multi.angle algorithms for estimating sea and land surface temperatures with ATSR data, International Journal of Remote sensing, 17 (11), 2089-2114.

[7] Sobrino, J.A., El-Kharraz, J. and Li, Z.L. (2003). Surface temperature and water vapour retieval from MODIS data. International Journal of Remote Sensing. 24 (24), 5161-5182.

[8] Sobrino, J.A, Raissouni, N and Li, Z.-L. (2001). Acomparative study of land surface emissivity retieval from NOAA data. Remote Sensing of Environment, 75, 256-266.

[9] Sobrino, J. A., Raissouni, N., Simarro, J., Nerry, F., and Petitcolin, F. (1999). Atmospheric water vapor content over land surfaces derived from the AVHRR data: Application to the Iberian Peninsula. IEEE, Transactions on Geoscience and Remote Sensing, 37, 1425−1434.

[10] Sobrino, J.A, Z.-L.Li, Stoll, M.p. and Becker, F. (1996). Multi.Channel and Multi.angle algorithms for estimating sea and land surface temperatures with ATSR data, International Journal of Remote sensing, 17 (11), 2089-2114.

[11] MSG Level 1.5 Image Data Format Description, Doc Nº: EUM/MSG/ICD/105, August 2007

[12] Sobrino, J.A. and Romaguera, M. (2004). Land surface temperature retrieval from MSG1-SEVIRI data. Remote Sensing of Environment, 92, 247-254

[13] Sobrino, J.A. and Romaguera, M. (2008). Water vapour retrieval from Meteosat 8/SEVIRI observations. International journal of remote sensing, 29:3, 741-754

[14] Radiometric Calibration of MSG SEVIRI Level 1.5 Image Data in Equivalent Spectral Blackbody Radiance, Doc Nº: EUM/OPS-MSG/TEN/03/0064, January 2007

[15] Typical Radiometric Accuracy and Noise for MSG-1/2, Doc Nº: EUM/OPS/TEN/07/0314, February 2007